



Volume 127

2025

p-ISSN: 0209-3324

e-ISSN: 2450-1549

DOI: <https://doi.org/10.20858/sjsutst.2025.127.5>



Journal homepage: <http://sjsutst.polsl.pl>

**Article citation information:**

Golchin, B., Raffi, M.A.B., Zakaria, N.Z., Abdullah, N.H. Pavement condition assessment using lidar and ArcGIS: an experience from Malaysia. *Scientific Journal of Silesian University of Technology. Series Transport*. 2025, **127**, 73-85. ISSN: 0209-3324.

DOI: <https://doi.org/10.20858/sjsutst.2025.127.5>

**Babak GOLCHIN<sup>1</sup>, Muhammad Aiman Badrish RAFFI<sup>2</sup>, Nur Zarifah ZAKARIA<sup>3</sup>,  
Noor Halizah ABDULLAH<sup>4</sup>**

**PAVEMENT CONDITION ASSESSMENT USING LIDAR AND  
ARCGIS: AN EXPERIENCE FROM MALAYSIA**

**Summary.** Pavements require regular maintenance due to the wear and tear caused by traffic loads and environmental conditions, which lead to various surface defects. This study explores the use of Light Detection and Ranging (LiDAR) technology and ArcGIS software to identify pavement defects in selected regions of Malaysia. The Jambatan Sultan Abdul Halim Muadzam Shah Expressway (JSAHMSE) and the Guthrie Corridor Expressway (GCE) were chosen as test sites for evaluating this approach. Initially, point cloud data were collected from both expressways using LiDAR, and related images were processed through ArcGIS software to identify defects on the road surfaces. The analysis revealed defects such as shoving, bleeding, longitudinal cracking, potholes, and patching on the GCE, while raveling, longitudinal cracking, bleeding, and edge cracking were observed on the JSAHMSE. Simultaneously, manual visual inspections were conducted, and defects were documented. A comparison of the results from both methods showed

<sup>1</sup> Department of Civil Engineering, University of Mohaghegh Ardabili, Ardabil, Iran. Email: [b.golchin@uma.ac.ir](mailto:b.golchin@uma.ac.ir). ORCID: <https://orcid.org/0000-0002-7329-1596>

<sup>2</sup> School of Housing, Building and Planning, Universiti Sains Malaysia, 11800 USM, Penang, Malaysia. Email: [aimanbadrish11@gmail.com](mailto:aimanbadrish11@gmail.com). ORCID: <https://orcid.org/0009-0004-0734-4874>

<sup>3</sup> School of Housing, Building and Planning, Universiti Sains Malaysia, 11800 USM, Penang, Malaysia. Email: [zarifahzakaria14@gmail.com](mailto:zarifahzakaria14@gmail.com). ORCID: <https://orcid.org/0009-0007-3519-4043>

<sup>4</sup> School of Housing, Building and Planning, Universiti Sains Malaysia, 11800 USM, Penang, Malaysia. Email: [nhalizah@usm.my](mailto:nhalizah@usm.my). ORCID: <https://orcid.org/0000-0001-6645-7204>. (Corresponding Author)

that LiDAR and ArcGIS effectively identified the types and sizes (length and surface area) of the defects. However, ArcGIS struggled to accurately measure the depth of certain defects, making it difficult to assess their severity in detail.

**Keywords:** pavement defects, LiDAR, Point cloud, ArcGIS software

## 1. INTRODUCTION

With technological advancements playing a vital role in our lives, exploring new methods for road construction and maintenance has become increasingly important. For example, Santosa et al. (2020) introduced a low-cost, in-vehicle pavement distress inspection system that utilizes semiautomatic data processing for airport pavement management [1]. This system significantly reduced both the time and costs associated with data collection. Similarly, Wu et al. (2019) developed an innovative approach for detecting road potholes using mobile point clouds and imaging [2]. Another technology gaining traction in this field is LiDAR, which is being utilized for data collection in road construction and maintenance. LiDAR uses pulsed laser light to measure distances to the Earth, enabling the precise collection of geometric and attribute information about various objects.

LiDAR technology operates similarly to radar (radio detection and ranging), allowing for the mapping of Earth's topographic features over large areas and the determination of elevation [3]. It uses pulses of laser light to measure distances to target objects, creating three-dimensional data by coordinating latitude, longitude, and elevation (x, y, and z). Inside the LiDAR device, a spinning mirror continuously rotates along its vertical axis to collect data. The time it takes for a laser pulse to reach a target and bounce back to the scanner determines the distance between the LiDAR device and the object. This process generates a 3D point cloud, transforming scanned areas into detailed 3D models. LiDAR is significantly more efficient and cost-effective than traditional survey methods. Data can be collected through three methods: airborne, terrestrial, and mobile scanning. Terrestrial laser scanners are mounted on tripods and gather data from a fixed position, while mobile scanners can capture data while in motion. Airborne scanning, also known as aerial terrestrial scanning, is carried out using helicopters or fixed-wing aircraft, allowing for the coverage of large areas quickly.

In recent years, many studies have explored the use of LiDAR technology in various applications. Zalama et al. (2011) demonstrated how effective LiDAR can be for identifying geometric features like hills and holes [4]. Similarly, Fu et al. (2013) conducted experiments showing that LiDAR can accurately detect features such as bumps and holes [5]. Shamayleh and Khattak (2003) highlighted that LiDAR data could also be used to capture specific elements of roadway inventories [6]. Yang (2018) applied LiDAR to scan the surfaces of concrete slabs in pavements [7], while Guo (2015) used the technology to map out road surface characteristics [8]. He (2017) focused on the strengths of airborne LiDAR for collecting highway inventory data, emphasizing its potential in large-scale projects [9]. Neupane (2019) pointed out that mobile LiDAR has the potential to enhance both the availability and quality of surface data [10], especially for extensive road networks, by automating data collection. Li (2015) introduced an innovative method for detecting roads using aerial LiDAR point clouds, adaptable to variations in road network intensity data [11]. Additionally, Puente (2013) compared the performance of mobile LiDAR with ground-coupled GPR (2.3-GHz antenna), offering insights into the relative strengths of each approach [12].

Other researchers have explored various innovative applications of LiDAR technology. Yadava et al. (2018) introduced an automated technique using Mobile Laser Scanning (MLS) to estimate road width, centerlines, longitudinal slopes, and cross slopes [13]. Jung (2019) took a different approach by breaking down LiDAR data into smaller sections using MLS and then converting it into a local coordinate system [14]. Martín-Jiménez (2018) focused on developing a method for analyzing LiDAR data, testing it on three sections of Spanish roads [15]. Holgado-Barco (2014), Yang (2013), and Kumar (2014) each proposed their own unique methods for processing and analyzing LiDAR data [16-18]. DiazVilarina (2016) highlighted that mobile laser scanning has been a reliable method for producing georeferenced point clouds and images, offering accurate and realistic representations of the environment [19]. Zhang (2019) developed an automated system for identifying and measuring road markings using 3D laser scanning data, which was later tested on real-world 3D data [20]. Yang (2018) emphasized the need for specialized software to support road design, expansion, and asset management, aiming to enhance the accuracy and effectiveness of road safety and management systems [21]. Saad and Tahar (2019) outlined a four-step process for evaluating ruts and potholes using LiDAR, covering site reconnaissance, data collection, data processing, and analysis [22]. Meanwhile, Akgul (2017) applied Terrestrial LiDAR to measure the rate of pavement deterioration due to changing weather conditions on forest roads [23].

Currently, highway departments around the world rely on pavement condition assessments to guide their maintenance efforts. In Malaysia, traditional methods for evaluating road conditions are still widely used, but they come with their challenges—they are costly, labor-intensive, and time-consuming, relying heavily on on-site measurements and visual inspections. These methods often only provide a limited view, with damage and deterioration detected through qualitative observations. However, as Ganendra (2018) points out, the precise terrain mapping capabilities of LiDAR have made it a popular choice in Malaysia for a range of applications, from engineering and infrastructure projects to environmental management, disaster response, and natural resource management [24]. This study explores how LiDAR data can be applied in road condition assessments, with a particular focus on identifying pavement issues more efficiently across Malaysia.

## **2. METHODOLOGY**

### **2.1. Study area**

Two sections were chosen for this study: the Jambatan Sultan Abdul Halim Muadzam Shah Expressway (JSAHMSE) and the Guthrie Corridor Expressway (GCE) in Malaysia. These locations were selected to evaluate and implement the LiDAR technology. Figure 1 provides actual images of both the GCE and JSAHMSE.

### **2.2. Instrument and Software**

In this research, LiDAR technology was utilized for data collection, while the Aeronautical Reconnaissance Coverage Geographic Information System (ArcGIS) served as the platform for analyzing the data. Developed by Esri, ArcGIS is a robust software for processing and managing maps and geographic data. After the data was collected in formats such as vector, raster, or LAS files, it was processed and visualized using ArcGIS to provide insights into pavement conditions.



Fig. 1. Actual image of GCE (left) and JSAHMSE (right)

### 2.3. Research Work

Figure 2 shows the flowchart of the research plan. The process began by applying a rectangular grid to map the coordinates of both expressways (see Figure 3). Next, road surface points were identified using 3-dimensional point clouds. In the initial stage, the LAS data points were divided into square grids of a predefined size. For each grid, planar ground points were extracted, which then served as the basis for identifying road points. A visual inspection of defects was carried out, and the necessary data was recorded and analyzed. Figure 4 provides a closer look at the LiDAR point clouds within the rectangular grid.

LAS data points are stored in the X-Y-Z-I format, which is an industry-standard binary format for airborne LiDAR data [25]. Here, XYZ represents the coordinates of each data point, while "I" indicates its intensity or strength. To project these data points onto a 2D plane, a rectangular grid is generated, grouping the data into a two-dimensional square map. The first step involves creating the LAS dataset in ArcGIS, which requires importing all relevant LiDAR data into a single, unified dataset. This dataset includes the point clouds collected from the GCE and JSAHMSE sections. Figure 5 offers a closer look at the 3D point clouds from these areas. Once the LAS dataset is created, the grid structure that aligns with the LiDAR data coordinates becomes visible.

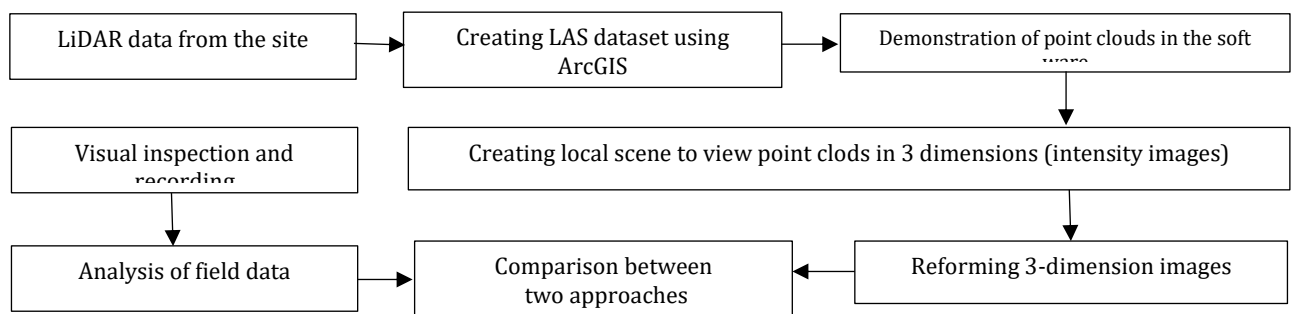


Fig. 2. Flow chart of research

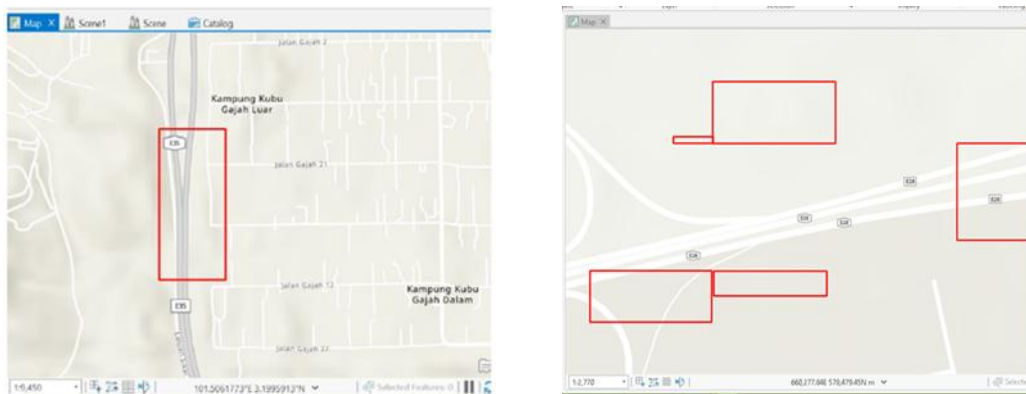


Fig. 3. Rectangular grid of the LAS dataset created with corresponding XY coordinates for GCE (left) and JSAHMSE (right)

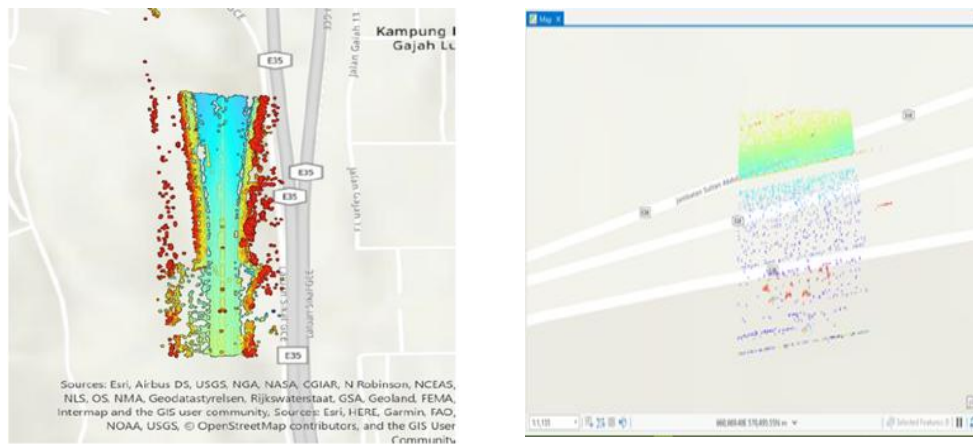


Fig. 4. A closer view of the LiDAR point clouds within the rectangular grid at the GCE (left) and JSAHMSE (right)

To visualize the point clouds, a new local scene is created in ArcGIS (New Map > New Local Scene). This 3D view allows for the identification of various elements within the expressway, such as light poles, advertisement boards, road barriers, and vegetation. The colors in the 3D model represent elevation changes, with red indicating higher elevations and green indicating lower ones (see Figure 6, left).

From these 3D perspectives, changes in elevation and identified objects appear as clusters of 3D points. It's worth noting that some objects detected on the expressway, like moving vehicles, may not be fully captured, resulting in partial data points. These can generally be disregarded when identifying road defects (see Figure 6, right). Figure 7 shows the west-east and north-south cross-sections of the GCE, providing a more detailed view of the data.

By analyzing the road profile generated from the LiDAR data, pavement failures can be identified by looking at the unevenness in the point clouds along the road surface. Additionally, changing the LiDAR point symbology from elevation to intensity images in the appearance tab of the LAS dataset layer makes these defects even more visible. Since LiDAR data tends to be quite large, converting it into intensity images helps to manage this bulkiness [26]. This conversion enhances the clarity, making it easier to spot issues on the pavement. Figure 8 displays the intensity images derived from LiDAR points for the GCE.

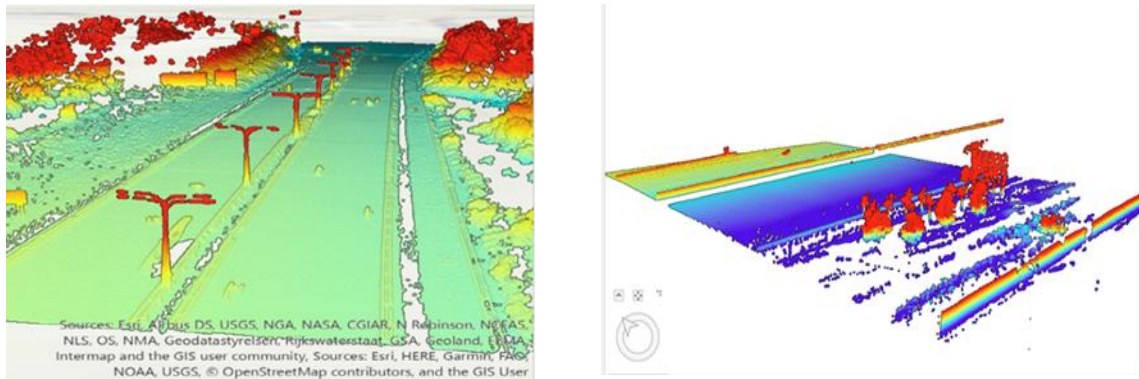


Fig 5. A closer view of the 3D point clouds of the GCE (left) and JSAHMSE (right)

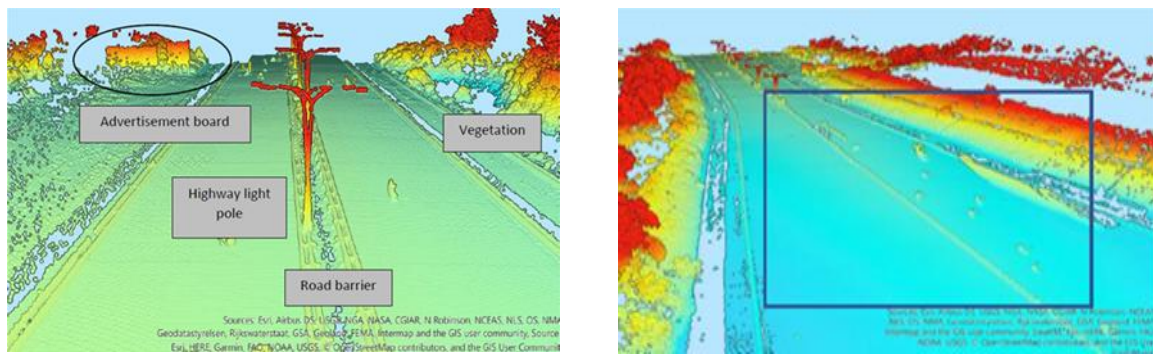


Fig. 6. Inventories of the GCE (left) and example of unclarified objects assuming as moving vehicles (Right)

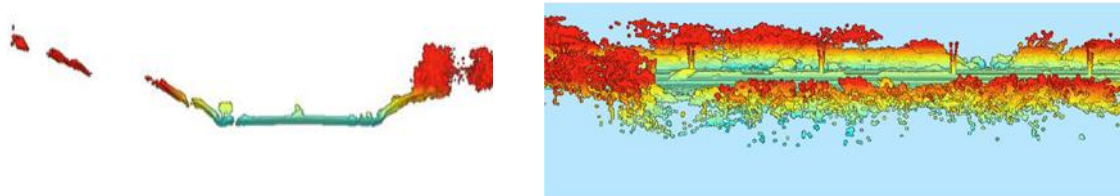


Fig. 7 The west-east cross-section (left) and north-south cross-section (right) of the GCE

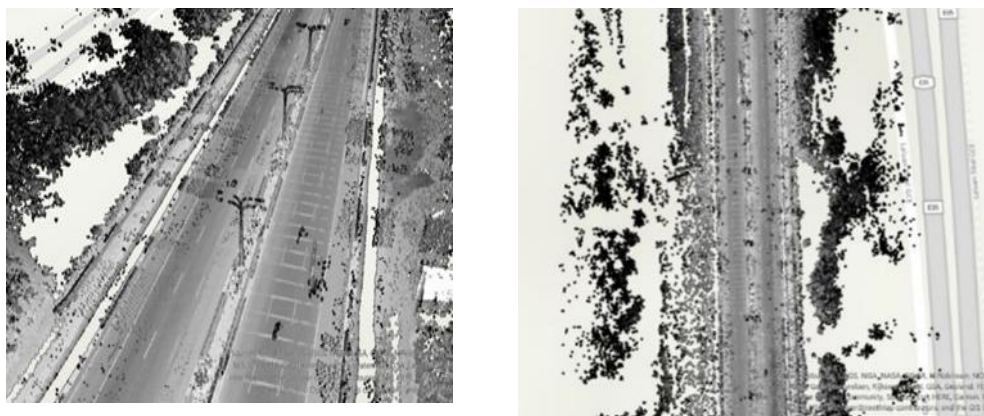


Fig. 8. Intensity image for GCE

### 3. RESULT AND DISCUSSION

#### 3.1. GCE pavement defects

In the selected section of the GCE, shoving was observed at coordinates 101.5076887°E, 3.1980663°N. Shoving occurs due to shear forces created by traffic, especially from vehicles that frequently start and stop. This results in the pavement surface shifting either longitudinally or transversely [27]. Other contributing factors include an unstable Hot Mix Asphalt (HMA) layer and excessive moisture in the subgrade. In this specific section, the shoving failure measures approximately 2.01 meters in length, 2.53 meters in width, covering a total area of 5.09 square meters (see Figure 9).

Bleeding on the pavement surface is characterized by a shiny, glass-like appearance (see Figure 9). In the images generated by ArcGIS, this type of failure appears as watery or paint-like patches scattered unevenly along a single wheel path. Two instances of bleeding were identified on the left lane of the analyzed expressway section, as shown in Table 1. Severe bleeding can pose a safety risk, as it may cause vehicles to skid when the surface is wet, leading to a loss of traction and control.

Tab. 1

Bleeding failures identified on the pavement at GCE

Bleeding A	Coordinate	101.5076942°E 3.1985882°N
	Length	7.07 m
	Width	0.77 m
	Area	5.44 m <sup>2</sup>
Bleeding B	Coordinate	101.5077149°E 3.1991318°N
	Length	5.26 m
	Width	0.69 m
	Area	3.63 m <sup>2</sup>

Longitudinal cracking refers to a type of crack that runs parallel to the pavement’s centerline or laydown direction. Based on the software analysis, this failure was identified as longitudinal cracking, as it appears directly along the vehicle wheel path. The crack in this section is located in the left lane and measures approximately 16.01 meters in length (see Figure 9). It extends from coordinates 101.5073871°E, 3.2019300°N to 101.5073904°E, 3.2017888°N.

Potholes form when a shallow, bowl-shaped depression develops in the pavement, extending from the asphalt layer down to the base course. They typically appear because of pavement fatigue, which leads to interlocking cracks, often referred to as alligator cracking [28]. According to the ArcGIS analysis, a pothole was identified in the left lane of the expressway, measuring approximately 0.80 meters in length, 1.35 meters in width, and covering an area of 1.08 square meters. Its location is pinpointed at coordinates 101.5072856°E, 3.2014945°N (see Figure 9).

The analysis revealed that the GCE section contains several patches of varying sizes, from small to large (see Figure 9). Table 2 highlights the patched areas identified on the pavement surface. Patching involves replacing and covering sections of pavement to repair earlier damage. While it addresses some issues, patching can also create uneven surfaces, leading to discomfort for road users due to increased roughness. Despite being a common repair method, patching is still classified as a type of road failure.

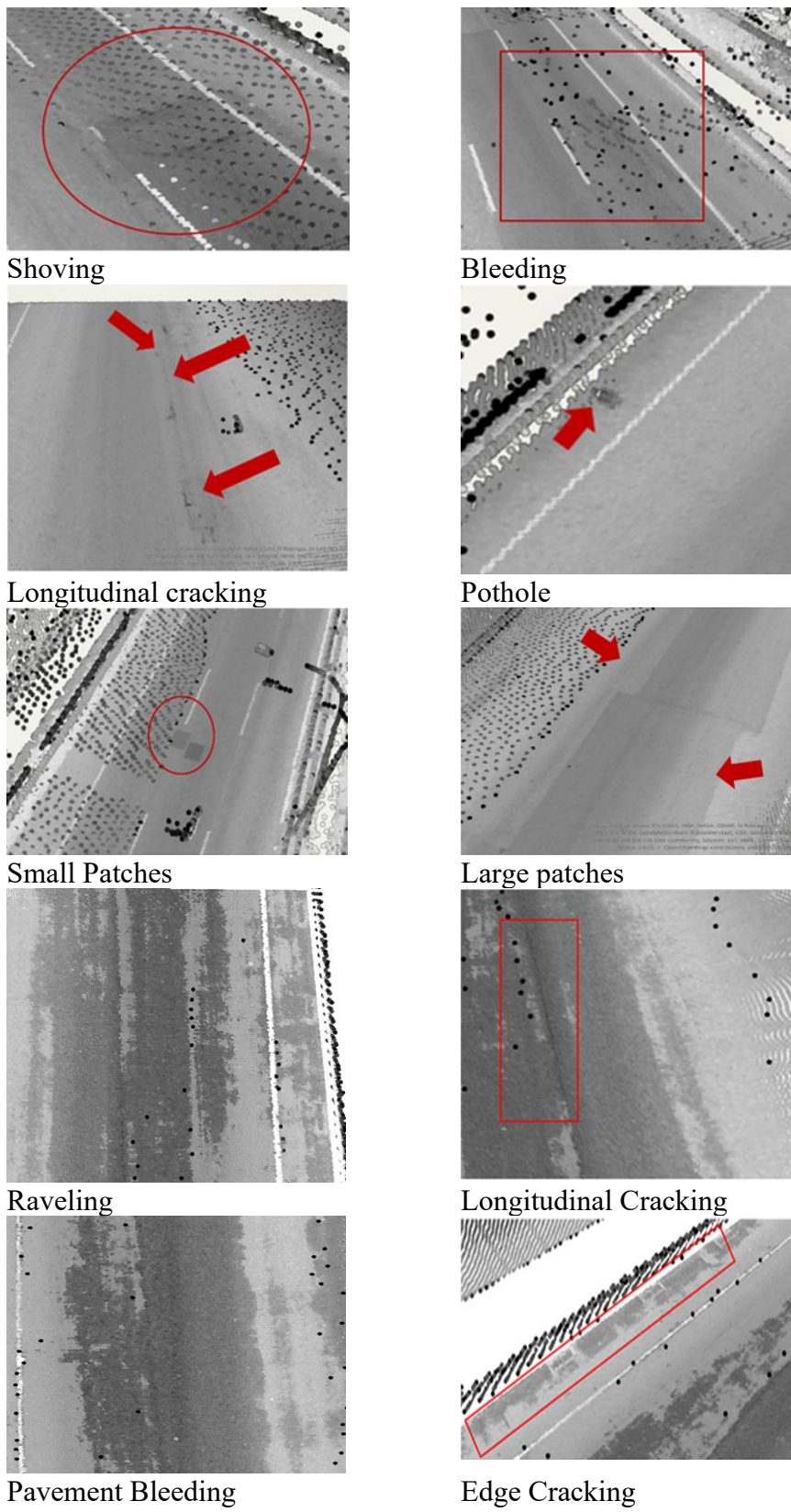


Fig. 9. Generated images for pavement defects from LiDAR and ArcGIS

Tab. 2

Patching identified on the pavement surface

Patching		
Coordinate	Measurement	
101.5074605°E 3.2000009°N	Length	2.13 m
	Width	1.38 m
	Area	2.94 m <sup>2</sup>
101.5074645°E 3.1998100°N	Length	2.87 m
	Width	1.25 m
	Area	3.59 m <sup>2</sup>
101.5074986°E 3.1979002°N	Length	1.20 m
	Width	1.12 m
	Area	1.34 m <sup>2</sup>
101.5075081°E 3.1978964°N	Length	1.18 m
	Width	1.02 m
	Area	1.20 m <sup>2</sup>
101.5076563°E 3.1987019°N	Length	49.76 m
	Width	3.65 m
	Area	181.62 m <sup>2</sup>
101.5077685°E 3.2011483°N to 101.5076931°E 3.1974416°N (end section)	Length	408.74 m to (end section)
	Width	10.12 m (start) 3.87 m (end)
101.5078300°E 3.2019525°N to 101.5077785°E 3.2011474°N (end section)	Length	97.77 m to (end section)
	Width	9.89 m (start) 10.35 m (end)

### 3.2. JSAHMSE pavement defects

Figure 9 shows the generated image of pavement raveling at JSAHMSE from the point cloud data. Raveling can be derived as a loss of fine and coarse aggregates from the asphalt matrix due to the adhesion failure at the interface. From the generated image, the pavement failure was measured, and it is 61.34 meters in length. The location of the failure was identified and coordinated from (100.4512780°E 5.2332425°N) to (100.4506732°E 5.2331457°N).

Figure 9 shows the generated image of longitudinal cracking at JSAHMSE based on point cloud data. Longitudinal cracking is a type of pavement distress that usually runs parallel to the edge of the pavement shoulder. According to the image, this crack measures approximately 9.75 meters in length, with its location pinpointed at coordinates 100.4511358°E, 5.2332338°N.

Figure 9 shows the generated image of pavement bleeding at JSAHMSE from point cloud data. However, the bleeding could also be mistaken for pavement raveling, as the image lacks clarity and the two types of damage appear similar. A more detailed inspection is required to accurately determine the type of pavement failure.

Figure 9 shows the generated image of edge cracking at JSAHMSE based on point cloud data. Edge cracking refers to cracks that run parallel to the pavement's edge, typically located 0.3 to 0.5 meters away from the edge. In this case, the severity appears to be low, as the cracks

are shallow and do not result in significant breaks or material loss. The affected area has already been repaired. Surface cracks are usually measured using longitudinal profiles, with the affected area calculated by multiplying the length of the defect by one meter. Defect density is then determined by dividing the affected area by the total scanned section area and multiplying by one hundred. However, in this study, the exact measurement of the failure could not be determined due to the unclear quality of the generated image. A more detailed site inspection is needed to accurately assess the extent and severity of the cracking.

#### 4. CONCLUSION

The process of analyzing LiDAR data to identify pavement failures using ArcGIS software involves three main phases: combining all available LAS data into a single dataset, creating a 3D view of the point clouds through a local scene in ArcGIS, and conducting section analysis to identify failures.

1. The LiDAR point cloud data for both the GCE and JSAHMSE were processed in ArcGIS, resulting in 2D and 3D images of the road sections. These images allowed for the identification of various pavement failures across the two expressways.
2. Using the 3D intensity images generated from the ArcGIS software, several types of pavement failures were identified, including shoving, bleeding, longitudinal cracking, potholes, patching, raveling, and edge cracking. Importantly, no critical or severe failures were detected that would significantly impact driving comfort on the GCE and JSAHMSE.
3. While the ArcGIS software successfully identified and analyzed the length, width, and area of the pavement failures, it faced challenges in accurately measuring the depth of these defects. This limitation may be due to the minimal depth difference between the surface and the base of the failures. Depth information is especially critical for maintenance activities like repairing potholes, but this could not be accurately captured with the software. Additionally, determining the exact types of pavement failures can be difficult due to the software's inability to produce higher-intensity data from the LAS dataset, leading to potential confusion between similar-looking defects. As a result, the identified failures may not fully reflect the actual conditions of the GCE and JSAHMSE sections.
4. Although the use of ArcGIS software for assessing pavement conditions is not entirely precise, it offers significant time and area coverage advantages, reducing the need for extensive on-site inspections. However, on-site evaluations remain necessary for a complete and accurate assessment of pavement conditions. Visual inspections of selected sections demonstrated that LiDAR is an effective tool for identifying road surface defects, making it a valuable method for pavement assessments.

#### References

1. Santos Bertha, Pedro G. Almeida, Ianca Feitosa, Débora Lima. 2020. "Validation of an indirect data collection method to assess airport pavement condition." *Case Studies in Construction Materials* 13. ISSN: 2214-5095.  
DOI: <https://doi.org/10.1016/j.cscm.2020.e00419>.

2. Wu Hangbin, Lianbi Yao, Zeran Xu, Yayun Li, Xinran Ao, Qichao Chen, Zhengning Li, Bin Meng. 2019. "Road pothole extraction and safety evaluation by integration of point cloud and images derived from mobile mapping sensors." *Advanced Engineering Informatics* 42: 100936. ISSN: 1474-0346. DOI: <https://doi.org/10.1016/j.aei.2019.100936>.
3. Chin Abby. 2012. "Paving the way for terrestrial laser scanning assessment of road quality." *M.Sc. Thesis*, Oregon State University.
4. Zalama Eduardo, Jaime Gómez-García-Bermejo, José Llamas, Roberto Medina. 2011. "An effective texture mapping approach for 3D models obtained from laser scanner data to building documentation." *Computer-Aided Civil and Infrastructure Engineering* 26(5): 381-392. ISSN: 1474-0346. DOI: <https://doi.org/10.1111/j.1467-8667.2010.00699.x>.
5. Fu Pengcheng, Jeremy D. Lea, James N. Lee, John T. Harvey. 2013. "Comprehensive evaluation of automated pavement condition survey service providers' technical competence." *International Journal of Pavement Engineering* 14(1): 36-49. ISSN: 1029-8436. DOI: <https://doi.org/10.1080/10298436.2011.643794>.
6. Shamayleh Huda, Aemal Khattak. 2003. "Utilization of LiDAR technology for highway inventory." In: *Proceedings of the 2003 Mid-Continent Transportation Research Symposium*. Ames, Iowa.
7. Yang Shuo, Halil Ceylan, Kasthurirangan Gopalakrishnan, Sunghwan Kim, Peter C. Taylor, Ahmad Alhasan. 2018. "Characterization of environmental loads related concrete pavement deflection behavior using Light Detection and Ranging technology." *International Journal of Pavement Research and Technology* 11(5): 470-480. ISSN: 1996-6814. DOI: <https://doi.org/10.1016/j.ijprt.2017.12.003>.
8. Guo Jenny, Meng-Ju Tsai, Jen-Yu Han. 2015. "Automatic reconstruction of road surface features by using terrestrial mobile lidar." *Automation in Construction* 58: 165-175. ISSN: 0926-5805. DOI: <https://doi.org/10.1016/j.autcon.2015.07.017>.
9. He Yi, Ziqi Song, and Zhaocai Liu. 2017. "Updating highway asset inventory using airborne LiDAR." *Measurement* 104: 132-141. ISSN: 1536-6359. DOI: <https://doi.org/10.1016/j.measurement.2017.03.026>.
10. Neupane Saurav R., Nasir G. Gharaibeh. 2019. "A heuristics-based method for obtaining road surface type information from mobile lidar for use in network-level infrastructure management." *Measurement* 131: 664-670. ISSN: 1536-6359. DOI: <https://doi.org/10.1016/j.measurement.2018.09.015>.
11. Li Yong, Bin Yong, Huayi Wu, Ru An, and Hanwei Xu. 2015. "Road detection from airborne LiDAR point clouds adaptive for variability of intensity data." *Optik* 126(23): 4292-4298. ISSN: 0030-4026. DOI: <https://doi.org/10.1016/j.ijleo.2015.08.137>.
12. Puente Iván, Mercedes Solla, Higinio González-Jorge, and Pedro Arias. 2013. "Validation of mobile LiDAR surveying for measuring pavement layer thicknesses and volumes." *Ndt & E International* 60: 70-76. ISSN: 0963-8695. DOI: <https://doi.org/10.1016/j.ndteint.2013.07.008>.
13. Yadav Manohar, Ajai Kumar Singh, and Bharat Lohani. 2018. "Computation of road geometry parameters using mobile LiDAR system." *Remote Sensing Applications: Society and Environment* 10: 18-23. ISSN: 23529385. DOI: <https://doi.org/10.1016/j.rsase.2018.02.003>.

14. Jung Jaehoon, Erzhuo Che, Michael J. Olsen, Christopher Parrish. 2019. "Efficient and robust lane marking extraction from mobile lidar point clouds." *ISPRS journal of photogrammetry and remote sensing* 147: 1-18. ISSN: 0924-2716. DOI: <https://doi.org/10.1016/j.isprsjprs.2018.11.012>.
15. Martín-Jiménez José Antonio, Santiago Zazo, José Juan Arranz Justel, Pablo Rodríguez-Gonzálvez, Diego González-Aguilera. 2018. "Road safety evaluation through automatic extraction of road horizontal alignments from Mobile LiDAR System and inductive reasoning based on a decision tree." *ISPRS journal of photogrammetry and remote sensing* 146: 334-346. DOI: <https://doi.org/10.1016/j.isprsjprs.2018.10.004>.
16. Holgado-Barco Alberto, Diego Gonzalez-Aguilera, Pedro Arias-Sanchez, Joaquín Martínez-Sanchez. 2014. "An automated approach to vertical road characterisation using mobile LiDAR systems: Longitudinal profiles and cross-sections." *ISPRS Journal of Photogrammetry and Remote Sensing* 96: 28-37. ISSN: 0924-2716. DOI: <https://doi.org/10.1016/j.isprsjprs.2014.06.017>.
17. Yang Bisheng, Lina Fang, Jonathan Li. 2013. "Semi-automated extraction and delineation of 3D roads of street scene from mobile laser scanning point clouds." *ISPRS Journal of Photogrammetry and Remote Sensing* 79: 80-93. ISSN: 0924-2716. DOI: <https://doi.org/10.1016/j.isprsjprs.2013.01.016>.
18. Kumar Pankaj, Conor P. McElhinney, Paul Lewis, Timothy McCarthy. 2014. "Automated road markings extraction from mobile laser scanning data." *International Journal of Applied Earth Observation and Geoinformation* 32: 125-137. ISSN: 15698432. DOI: <https://doi.org/10.1016/j.jag.2014.03.023>.
19. Díaz-Vilariño L., H. González-Jorge, M. Bueno, P. Arias, I. Puente. 2016. "Automatic classification of urban pavements using mobile LiDAR data and roughness descriptors." *Construction and Building Materials* 102: 208-215. ISSN: 0950-0618. DOI: <https://doi.org/10.1016/j.conbuildmat.2015.10.199>.
20. Zhang Dejin, Xin Xu, Hong Lin, Rong Gui, Min Cao, Li He. 2019. "Automatic road-marking detection and measurement from laser-scanning 3D profile data." *Automation in Construction* 108: 102957. ISSN: 09265805. DOI: <https://doi.org/10.1016/j.autcon.2019.102957>.
21. Yang Mengmeng, Youchuan Wan, Xianlin Liu, Jingzhong Xu, Zhanying Wei, Maolin Chen, Peng Sheng. 2018. "Laser data based automatic recognition and maintenance of road markings from MLS system." *Optics & Laser Technology* 107: 192-203. ISSN: 00303992. DOI: <https://doi.org/10.1016/j.optlastec.2018.05.027>.
22. Saad Azri Mat, Khairul Nizam Tahar. 2019. "Identification of rut and pothole by using multirotor unmanned aerial vehicle (UAV)." *Measurement* 137: 647-654. ISSN: 1536-6359. DOI: <https://doi.org/10.1016/j.measurement.2019.01.093>.
23. Akgul Mustafa, Huseyin Yurtseven, Serdar Akburak, Murat Demir, Hikmet Kerem Cigizoglu, Tolga Ozturk, Mert Eksi, Anil Orhan Akay. 2017. "Short term monitoring of forest road pavement degradation using terrestrial laser scanning." *Measurement* 103: 283-293. ISSN: 1536-6359. DOI: <https://doi.org/10.1016/j.measurement.2017.02.045>.
24. Ganendra T.R., E.T. Mobarakeh, S.M. Khalid. 2018. "Technical challenges of airborne LiDAR surveying technology in Malaysia." In: *IOP Conference Series: Earth and Environmental Science*.
25. ESRI. (n.d.). What is a LAS dataset? ArcGIS Pro Documentation. Retrieved June 16, 2021. Available at: <https://pro.arcgis.com>.

26. Husain Arshad, Rakesh Chandra Vaishya. 2018. "Road surface and its center line and boundary lines detection using terrestrial Lidar data." *The Egyptian Journal of Remote Sensing and Space Science* 21(3): 363-374. ISSN: 1110-9823.  
DOI: <https://doi.org/10.1016/j.ejrs.2017.12.005>.
27. Sorum Neero Gumsar, Thangmuansang Guite, Nungleppam Martina. 2014. "Pavement distress: a case study." *International Journal of Innovative Research in Science, Engineering and Technology* 3(4): 274-284. ISSN: 2347-6710.
28. Schnebele E., Burak F. Tanyu, Guido Cervone, N.J. Waters. 2015. "Review of remote sensing methodologies for pavement management and assessment." *European Transport Research Review* 7: 1-19. ISSN: 18668887.  
DOI: <https://doi.org/10.1007/s12544-015-0156-6>.

Received 22.03.2025; accepted in revised form 15.05.2025



Scientific Journal of Silesian University of Technology. Series Transport is licensed under a Creative Commons Attribution 4.0 International License